JP6J.4

THE STRUCTURE AND DYNAMICS OF ATMOSPHERIC BORES AND SOLITONS AS DETERMINED FROM REMOTE SENSING AND MODELING EXPERIMENTS DURING IHOP

Steven E. Koch, Mariusz Pagowski[1,2], James W. Wilson[3], Frederic Fabry[4], Cyrille Flamant[5], Wayne Feltz[6], Geary Schwemmer[7], and Bart Geerts[8]

[1] *NOAA Research – Forecast Systems Laboratory, Boulder, Colorado*
[2] *Cooperative Institute for Research in the Atmosphere, Colorado State University*
[3] *National Center for Atmospheric Research*
[4] *Radar Observatory, McGill University*
[5] *Institut Pierre-Simon Laplace, Paris, France*
[6] *Cooperative Institute for Meteorological Satellite Studies, University of Wisconsin*
[7] *NASA Goddard Space Flight Center*
[8] *Department of Atmospheric Sciences, University of Wyoming*

1. Introduction

Solitary waves are a class of gravity waves consisting of a single elevation of finite amplitude that, owing to a balance between nonlinearity and dispersion, propagates without change of form. A family of solitary waves, which is termed a "soliton", forms as the natural consequence of the evolution of a bore – a type of gravity wave (hydraulic jump) generated as a density current (such as cold air from a thunderstorm) intrudes into a fluid of lesser density, which in the case of the atmosphere, occurs beneath a low-level inversion. These phenomena were observed repeatedly by a multitude of ground-based and airborne remote sensing systems during the six-week field phase of the International H_20 Project (IHOP), even though bores were not one of the primary IHOP objectives (Weckwerth et al. 2004). These observing systems together produced the most extensive set of observations ever collected of the evolving structure of bores, solitons, and solitary waves. In spite of this, a more complete understanding of the dynamics of these phenomena and their interactions required use of very high-resolution numerical weather prediction models initialized with IHOP data. These observations and the numerical modeling together offer the opportunity for an unprecedented study of the evolving structure of bores, solitons, and solitary waves.

Corresponding author address: *Steven E. Koch, NOAA/OAR/FSL, R/FS1, 325 Broadway, Boulder, CO 80305-3328; e-mail <* Steven.Koch@noaa.gov*>*

2. Background material on bores

The presence of low-level stratification favors the ordered evolution of gravity currents into turbulent bores, bores, solitons, and finally solitary waves (Christie et al. 1979; Simpson 1987). One characteristic of gravity currents is a "feeder flow" of air directed from behind the head of the gravity current toward its leading edge in a current-relative framework. Passage of gravity currents at a ground site is usually identifiable by an abrupt pressure jump hydrostatically related to the mean cooling throughout the depth of the current, a sharp wind shift caused by the horizontal gradient of the pressure perturbation field, and increased gustiness due to strong vertical mixing in the head.

An internal bore in the atmosphere is a type of gravity wave disturbance that propagates on a low-level inversion ahead of gravity currents. Bores typically are generated as a gravity current intrudes into a stably-stratified boundary layer (SBL) of sufficient depth near the ground, resulting in a sustained elevation of the inversion layer. Amplitude-ordered solitary waves (a train of which is referred to as a soliton) can evolve from bores in some instances. Because the speed of a solitary wave is proportional to the wave amplitude, a dispersive family of waves evolves from the initial bore with amplitudes inversely related to their widths. The number of waves increases continuously with time to a finite value, though the number of waves is highly dependent upon the turbulent dissipation.

According to the hydraulic theory of Rottman and Simpson (1989), hereafter RS89, bore propagation speed depends upon its depth (d_b), the SBL inversion depth (h_0), and the speed of a long gravity wave (C_{gw}) as follows:

$$C_{bore} \Big/ C_{gw} = \left[0.5 \left(d_b / h_0 \right) \left(1 + d_b / h_0 \right) \right]^{1/2} . \qquad (1)$$

Koch and Clark (1999) have applied other predictive equations for bore speed to account for such factors as finite fluid depth, vanishingly small depth of the stable layer, and energy loss restricted to the neutral layer above the SBL waveguide (Klemp et al. 1997). In general, the SBL must be sufficiently deep and intense to support a bore of a given strength. The modeling work of Haase and Smith (1989b), hereafter HS89, and Jin et al. (1996) sheds light on this issue. HS89 suggest that two parameters govern whether an undular bore will be generated from an intrusive gravity current:

$$F = \frac{\left(U - C_{gc} \right)}{C_*} = \frac{\left(U - C_{gc} \right)}{\sqrt{g \, \Delta\theta \, d_{gc} / \theta_{vw}}}$$

and (2)

$$\mu = \frac{C_0}{C_{gc}} = \frac{2 N h_0 / \pi}{C_{gc}}$$

The first parameter F is the ratio of the front-relative "inflow velocity" of the cold air (U - C_{gc}) to the densimetric speed of a gravity current (C^*), the latter being a function of the gravity current depth d_{gc} and temperature contrast (μ). The second parameter is the ratio of the long gravity wave phase speed C_0 to the gravity current speed (C_{gc}). Note that C_0 depends upon the inversion layer strength (N) and depth (h_0). The parameter μ determines whether an undular bore (or solitary wave) will form and propagate ahead of the gravity current as required. When μ<0.7 (the "supercritical regime"), the gravity current propagates faster than any gravity waves and a well-defined feeder flow is present. When the value of μ increases to near 0.7, but still within this supercritical regime, undular bores may form. Bores and solitary waves are spawned when μ>0.7 (the "subcritical regime") as the gravity wave propagates considerably faster than the gravity current. For large values of F, several well-defined solitary waves may propagate ahead of the gravity current.

This prediction for the strength of a bore may be compared to another one based upon hydraulic theory and the laboratory work of RS89, which does not require knowledge of the inflow velocity, but instead depends upon:

$$Fr = \frac{C_{gc}}{C_{gw}} = \frac{C_{gc}}{\left(g \, \delta\theta \, h_0 / \theta_{vw} \right)^{1/2}} = \frac{C_{gc}}{N h_0}$$

and (3)

$$H = \frac{d_{gc}}{h_0}$$

where Fr is the Froude number, H is a measure of the depth of the gravity current to the inversion depth, and the potential temperature change across the inversion is given by $\delta\theta$. It is of some interest to note that the Froude number used in RS89 is proportional to the inverse of the μ parameter used in HS89, i.e., the critical value μ>0.7 equates in the RS89 nomenclature to:

$$\frac{C_{gc}}{N h_0} < \frac{2}{\pi \mu_c} = 0.91 . \qquad (4)$$

The presence of the gravity current is no longer critical to the evolution of the undular bore and solitary waves once the bore has been generated (Christie 1989). In the simplest case, the bore is generated on top of a surface-based, pre-frontal stable layer of sufficient depth as the gravity current intrudes into the SBL. In the real atmosphere, complex stratification, vertical wind shear, elevated inversions, and unsteady and/or multiple gravity currents may complicate matters. In addition, the PBL must be sufficiently deep and intense to support a bore of a given strength (Rottman and Simpson 1989). If a mechanism is not present to trap the vertical propagation of wave energy, the bore will quickly diminish (Crook 1988; Koch et al. 1991; Koch and Clark 1999). Wave trapping ability is typically measured by the Scorer parameter defined as:

$$m^2 = \frac{N_m^2}{\left(U - C_{bore} \right)^2} - \frac{\partial^2 U / \partial z^2}{\left(U - C_{bore} \right)} - k^2 , \qquad (5)$$

where k and m are the horizontal and vertical wavenumbers, N_m is the moist Brunt-Väisälä frequency, U is the background wind in the direction of bore propagation, and C_{bore} is the bore propagation speed. A rapid decrease of m with height supports wave trapping. Of particular relevance to bores is the low-level jet mechanism, which seems to be quite prevalent in bore case studies (Koch et al.1991), since it gives rise to strong trapping related to curvature in the velocity profile (the second term in the Scorer equation).

Koch and Clark (1999) provide a methodology for determining whether observed phenomena are gravity currents, bores, or solitary waves. The minimum requirements that must be satisfied to support the hypothesis that a phenomenon is actually a gravity current are that:

- Its depth as predicted hydrostatically using gravity current theory agrees with that measured by the remotely sensed data.
- Its speed of propagation observed prior to deceleration is consistent with that predicted from gravity current theory.
- A region of pronounced positive front-relative "feeder flow" is observed behind the leading edge of the gravity current above the surface layer (so as to minimize frictional effects).

Requirements that must be satisfied to support the hypothesis that a phenomenon is an internal bore are that:

- Its depth and speed of propagation are consistent with that of a bore of at least moderate intensity.
- The predicted bore depth is comparable to that derived from the observations.

"Bore intensity" is defined as the ratio of the mean bore depth to the SBL depth (h_1/h_0). Smooth (undular) bores are observed in the laboratory for $1 < h_1/h_0 < 2$; strong bores are turbulent and occur for $2 < h_1/h_0 < 4$; and for even larger values, the bore appears more like a gravity current because a very shallow inversion has little influence. These values follow from hydraulic theory, which predicts the kind of disturbance that may be forced as gravity currents encounter a surface-based SBL (Rottman and Simpson 1989).

It can be difficult to distinguish bores from gravity currents, and solitons from bores. Bores and gravity currents are both accompanied by a windshift into the direction of movement of the disturbance associated with a sudden pressure jump, and a net cooling in the lower troposphere. The degree of cooling should be hydrostatically consistent with the sustained surface pressure increase that follows an initial abrupt pressure jump, as recorded in sensitive surface microbarograph data. Cooling associated with gravity currents is due primarily to horizontal advection of the denser air, whereas adiabatic ascent is the cause of cooling in the case of a bore. Thus, pronounced surface cooling is not characteristic of bores; in fact, weak warming (and drying) may occur as the result of turbulent downward mixing of warmer (and typically drier) air from above the inversion into the SBL.

Gravity currents may generate other kinds of gravity waves besides bores and solitary waves. Model simulations show that a broad spectrum of gravity waves may be produced by gravity currents, including trapped lee-type waves created by strong flow over the head of the gravity current (Jin et al. 1996). Trapped lee waves display no vertical tilt and are motionless relative to the gravity current head. Lee-wave trapping occurs only under a very special condition in which the Scorer parameter decreases sufficiently rapidly with height. Kelvin-Helmholtz waves may also be produced in a thin region of strong vertical wind shear between the body of cold air in the gravity current and the air above it (Droegemeier and Wilhelmson 1985; Mueller and Carbone 1987). Kelvin-Helmholtz waves propagate rearward relative to the gravity current head, in contrast to trapped lee waves behind the gravity current head.

Intermediate structures between a pure gravity current and a smooth undular bore have been studied in the laboratory (Maxworthy 1980), simulated with idealized numerical models (Haase and Smith 1989a,b), and suggested in observational case studies (Fulton et al. 1990; Locatelli et al. 1998). As the gravity current begins to intrude into a stably stratified fluid, the fluid first envelops the head of the gravity current and then begins to move away from the gravity current head as an incipient bore, carrying a remnant of the cold air originally contained in the gravity current within a closed circulation at the leading edge of the bore in the form of a solitary wave. Laboratory experiments have shown that a family of solitary waves (soliton) develop and propagate ahead of the gravity current as the current slows down, but only when a stable waveguide is present at low

levels. Numerical simulations similarly reveal that, as the gravity current slows down with time in association with a decrease of the current depth, the current head becomes separated from the body of the current and resembles a large amplitude wavelike disturbance, with cold air contained within the closed circulations.

3. Instrument description

A large number of instruments at the Homestead Profiling Site in the Oklahoma Panhandle were used for the following purposes in this study: boundary layer height fluctuations from an FM-CW radar (Ince et al. 1998), horizontal and vertical winds from the NCAR Multiple Antenna Profiler (MAPR, Cohn et al. 2001), moisture and temperature profiles from an Atmospheric Emitted Radiance Interferometer (AERI, Feltz et al. 2003) at 20-min intervals, detailed sounding capability at 3-h intervals from the NCAR Integrated Sounding System (ISS) and CLASS systems, and detailed measurements of winds, moisture, and temperature fluctuations from a collection of surface mesonetworks. The NCAR S-POL radar (Lutz et al. 1995) provided reflectivity, radial velocity, and low-level fields of derived refractivity (Fabry et al. 1997). A Scanning Raman Lidar (SRL, Demoz et al. 2003), the GLOW Doppler lidar (Gentry et al. 2000), and an aerosol backscatter lidar (HARLIE, Schwemmer et al. 1998) respectively provided water vapor, aerosol, and wind data at high resolution. Aircraft data used here consisted of moisture measurements from the Leandre-II Differential Absorption Lidar (DIAL) aboard the NRL P-3 aircraft (Bruneau et al. 2001), and in situ meteorological measurements from the University of Wyoming King Air (UWKA).

4. Numerical model configuration

There were perhaps as many as 18 documented bores during the six-week IHOP field phase. Two bores on 4 June 2002 and a third one on 20 June 2002 are discussed in this paper. As discussed below, the bore on 20 June was produced by a thunderstorm outflow boundary propagating along a surface cold front. Bore A on 4 June was generated by an advancing outflow boundary acting as a gravity current, whereas bore B (which occurred 4h later) was generated along a southward-advancing cold front (the parent gravity current likely having been enhanced by post-frontal convection).

MM5 numerical simulations of the 4 June bore event were performed, but not of the 20 June case. The MM5 model employed one-way nested grids with resolutions of 18, 6, 2, and 0.7 km, with initial and boundary conditions for the coarsest grid being specified by the operational 20-km Rapid Update Cycle (RUC) model. All four nests contained 44 vertical levels, half of which were contained in the lowest 1.5 km of the atmosphere.

The Kain-Fritsch cumulus parameterization was employed on the 18-km grid, but not on the finer grids, in all cases except the BT control run, which used the Grell-Devenyi scheme; the latter cumulus parameterization scheme is employed in the RUC model. The Reisner mixed-phase microphysics scheme was utilized on all the grids. The RRTM radiation scheme used in the Weather Research and Forecasting (WRF) system and as default for the MM5 system was used.

Three different planetary boundary layer (PBL) experiments were performed, all of which employ the Mellor-Yamada 2.5 closure: the Burk and Thompson (1989) scheme (“BT”), the Eta model PBL scheme (Janjic 1994), and the Kantha and Clayson (1994) “QL” scheme. The BT scheme, which uses a diagnostic mixing length approach, served as the control, since it acts as the PBL scheme in the RUC model. The Eta PBL scheme is similar to the BT scheme, except it limits the size of the mixing length in statically stable layers, resulting in generation of less Turbulent Kinetic Energy (TKE). The QL scheme utilizes prognostic equations for TKE and mixing length, offers an improved closure for the pressure covariance term in the TKE equation, and most importantly, a Richardson number-dependent shear instability mixing term in strongly stratified layers (which enhances TKE in stable layer above a well-mixed PBL, such as might be encountered in the case of bores). We emphasize the results using the BT scheme in this paper.

5. The 20 June 2002 bore

A spectacular bore and its evolution into a beautiful amplitude-ordered train of solitary waves was sampled during the early morning hours of 20 June 2002 by the Leandre-II aboard the P-3 aircraft and a number of ground-based observing

systems – notably the S-POL radar, which captured the existence of an intense, but very shallow low-level jet atop the bore. The origin of this bore was traceable to a propagating cold outflow boundary from a mesoscale convective system in extreme western Kansas shortly before 0300 UTC. The existence of the outflow boundary was first made known by the appearance of a "fine line" in the WSR-88D composite radar displays. As the outflow boundary expanded and propagated southeastward, the gravity current encountered a strong surface-based stable layer and low-level jet, and generated a bore and solitary wave train.

The S-POL radar detected 5–6 waves with a horizontal wavelength of 11 km as the bore approached the Homestead vicinity (Fig. 1). The vertical structure of the bore seen in range-height indicator (RHI) displays of reflectivity and radial velocity (Fig. 2) suggests trapped waves lacking any discernible vertical tilt in the lowest 2 km of the atmosphere. Also apparent in these vertical cross sections is a very strong (24 m s^{-1}) southerly jet riding along the top of the solitary wave train. The ISS sounding taken at 0602 UTC also showed a similar 22 m s^{-1} jet at 1.5 km MSL. The presence of this remarkably strong, but shallow, low-level jet should have a significant influence on the curvature term in the Scorer parameter, resulting in wave trapping.

This suggestion of wave trapping is supported by the Leandre-II DIAL measurements taken from an altitude of 4.5 km MSL (Fig. 3). Although the wave train exhibits pronounced changes with each successive aircraft pass through the system, the consistent lack of any discernible wave tilt with height is a direct indication of wave trapping. On the first overpass (0329–0352 UTC), solitary waves with a horizontal wavelength of 15 km are apparent following the continuous rise in the height of the moist inversion layer from its undisturbed value of 1.3 km MSL to its displaced altitude of 2.5 km. On the second overpass (0408–0427 UTC), the same solitary wave features appear in the data, though with less of a stair step rise than before. Amplitude ordering of the waves is quite obvious. On the third overpass (0555–0616 UTC), which is when the ground observing systems at Homestead were intensively following the bore, perhaps the most beautiful of all the solitons during IHOP was seen. Approximately nine waves are present; these waves display a spacing of 12 km, but lack the amplitude-ordering seen earlier. On the contrary, the inversion surface is lifted successively higher with each passing wave, from 1.3 km to 1.7 km, and eventually to 2.1 km. These observations suggest that the flattening of the leading wave in the wavetrain brought about the demise of the soliton. Finally, note the existence of mirrored oscillations at 3.2 km altitude in phase with those much lower: these features are likely clouds induced by the lifting at lower levels.

5. The 4 June 2002 bores

Two other bores were sampled by IHOP remote sensing systems during the early morning of 4 June 2002. Bore A was generated by an outflow boundary from dissipating thunderstorms in extreme eastern New Mexico, which crossed the Oklahoma Panhandle, reaching the Homestead network at ~0630 UTC. Bore B developed in association with a southward-advancing cold front, likely enhanced by postfrontal convection in northwestern Kansas, and reached the Homestead area at ~1030 UTC. The bores were well sampled by the ground-based systems at Homestead.

Bore A is quite impressive in the FM-CW and MAPR (Fig. 4) and the HARLIE displays (Fig. 5). At this stage, the bore had the character of a soliton composed of waves with horizontal wavelength of ~10 km, consistent with the S-POL radar reflectivity imagery (not shown). The influence of the bore is felt as high as the top of the MAPR data (to at least 3 km). Bore B was characterized by at least 6 waves with a similar period of 15-20 min (not shown). In both cases, a quadrature phase relation between the vertical motions and the oscillations of the inversion surface supports the solitary wave interpretation of these data. HARLIE shows more clearly the multiple stratified layers perturbed by the solitary wave disturbances. The original SBL at 0.7 km was incrementally elevated to a height of 1.2 km following the second wave in the soliton. A 3-layer atmospheric structure is seen by all three observing systems, but the HARLIE most clearly reveals the lifting by the bore of the less strongly defined layer from 1.0 to ~ 2.1 km and lifting of the third layer from ~ 2 to ~ 4 km.

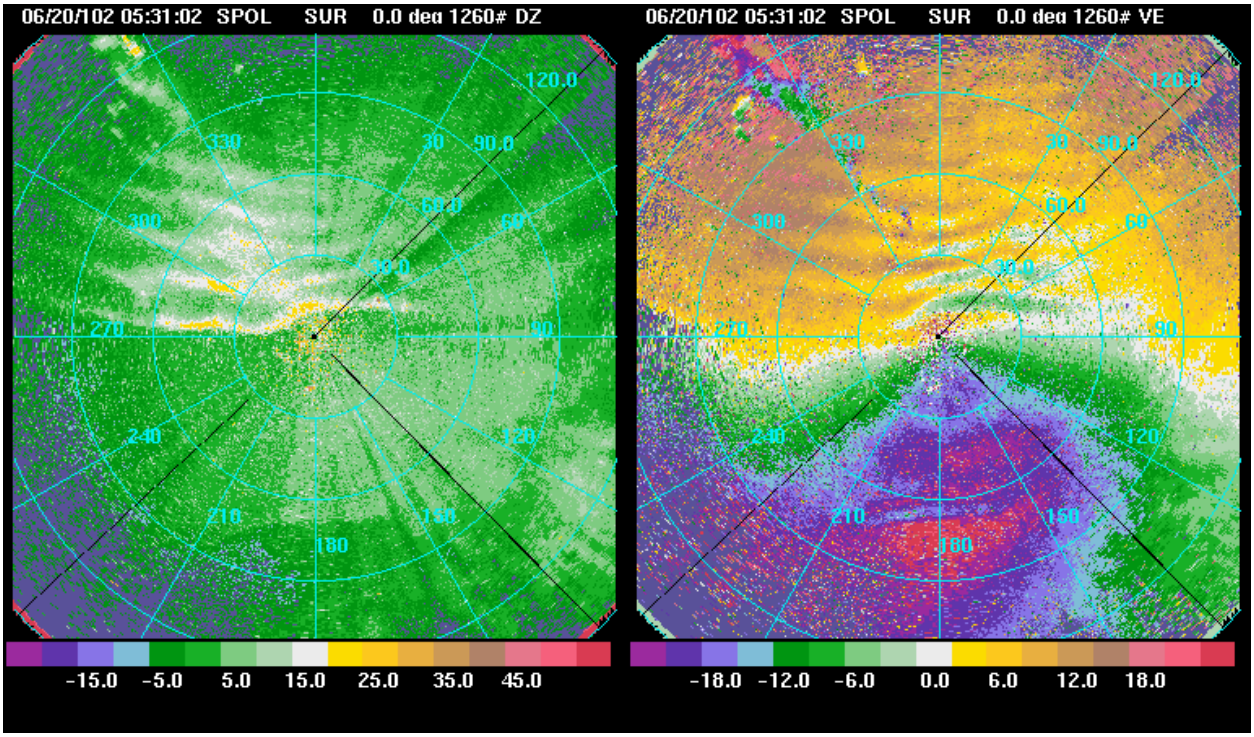

Fig. 1. Bore and trailing solitary wave train as seen in S-POL imagery at 0531 UTC 20 June 2002 of (left) radar reflectivity factor (dBZ), and (right) radial velocity (m s^{-1}). Positive radial velocities (warm colors) are directed away from the radar. Range rings are at 30-km spacing.

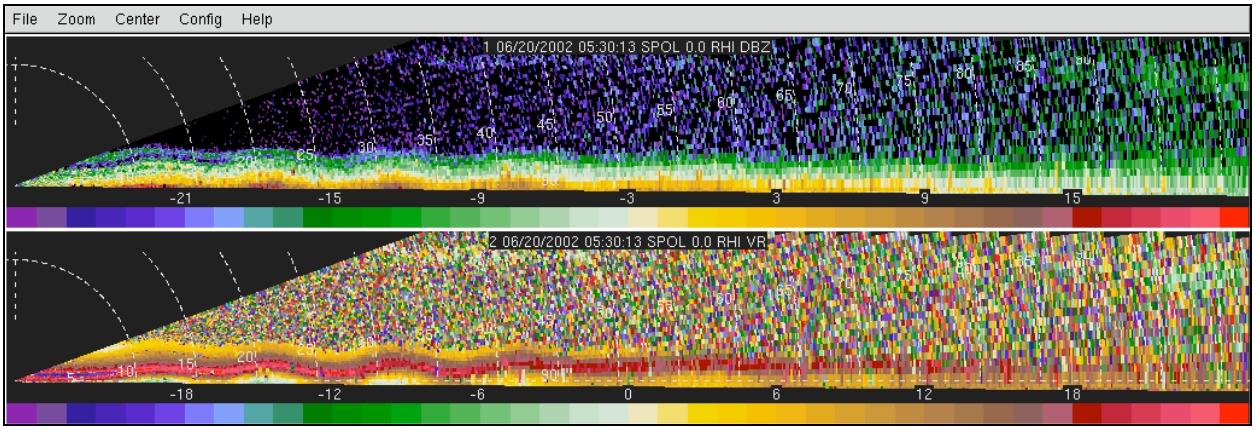

Fig. 2. Range-height indicator (RHI) displays of (top) S-POL radar reflectivity (dBZ) and (bottom) radial velocity (m s^{-1}) showing vertical structure of solitary wave train and very strong (> 20 m s^{-1}) southerly jet at 2 km AGL at 0530 UTC (for direct comparison with Fig. 1). Horizontal wavelength is 11 km (dashed white lines indicate range from radar). RHI is directed due northward from radar (north is to the right).

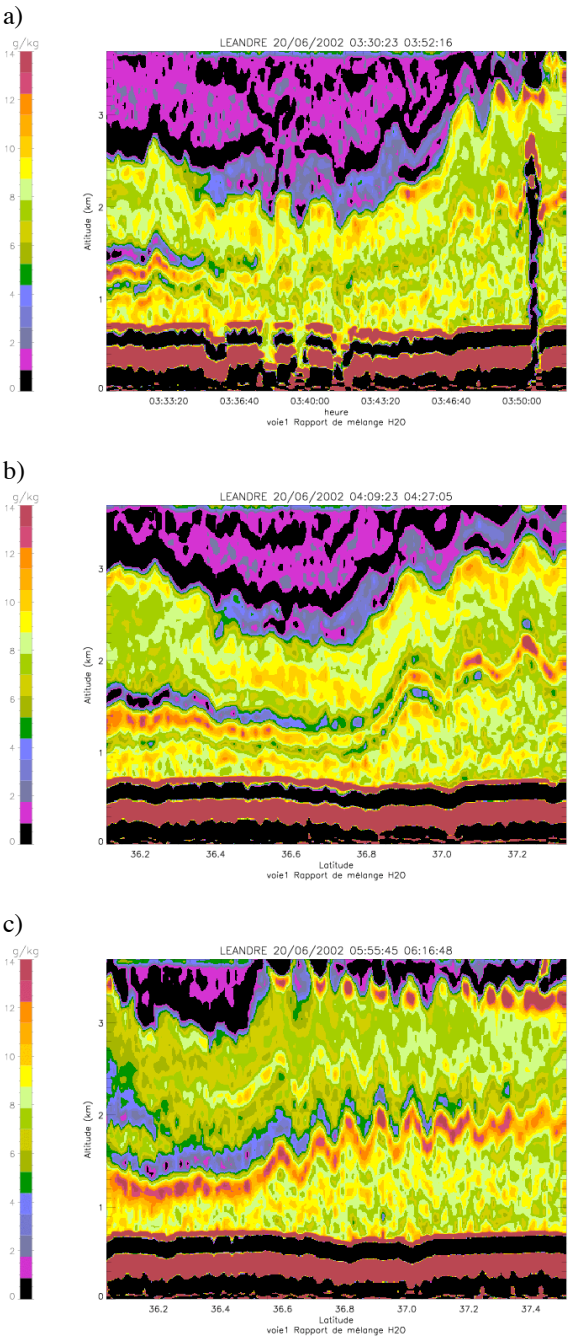

Fig. 3. Vertical cross sections of water vapor mixing ratio acquired with the Leandre-II DIAL system on three successive north-south interceptions of an evolving bore – solitary wave system: a) 0329–0352 UTC, b) 0408–0427 UTC, and c) 0555–0616 UTC.

The MAPR data were used to examine the influence of the bore lifting on the atmosphere so as to determine its ability to generate deep convection. Maximum updrafts below 2 km average ~1 m s^{-1} over the 10-min bore lifting periods, resulting in 600 m of lifting, which is in agreement with the observed increase of the SBL depth as seen in the FM-CW, MAPR and HARLIE displays. The MAPR data suggest that most of the lifting is contained below 2 km, indicating that wave energy is not propagating upward, and that waves dampen in the near-neutral layer above the SBL, as also suggested by HARLIE. Application of these layer displacement profiles to the special CLASS soundings taken in the Homestead vicinity (not shown) did not result in air parcels attaining their Level of Free Convection (LFC) because the lower troposphere was very dry. Deep convection was not actually initiated by bore A.

AERI measurements taken during the passage of the two bores indicated a sudden cooling and moistening aloft with no attendant near-surface cooling, a characteristic of bores. Likewise, the UWKA in-flight measurements of bore B detected 3C of cooling and 4 g kg^{-1} of moistening as the aircraft passed through the upper parts of the wave crests at a flight altitude of 1850 m AGL (Fig. 6). In addition, the aircraft data show a quadrature phase relation between fluctuations in potential temperature and vertical motions, with updrafts leading cooling periods, and vice versa; this is a behavior expected for gravity waves (solitary waves). The magnitude of the vertical motions is 1 – 2 m s^{-1}, similar to that seen in the MAPR data for bore A.

The near-surface refractivity fields computed from the S-POL (Fabry et al. 1997) show the existence of a pronounced band of reduced refractivity associated with the leading edge of bore A (Fig. 7). Refractivity may be reduced by warming and/or drying, as shown by its mathematical formulation:

$$N = 3.73\times10^{5}\frac{e}{T^{2}} + 77.6\frac{P}{T} \qquad (6)$$

A decrease in refractivity of 7 units, as seen in Fig. 7 accompanying the bore, can easily be produced by a decrease in moisture vapor pressure (*e*). The S-POL derived changes in refractivity are quite consistent with computed changes from the NCAR mesonet station time series data for bore A (Fig. 8b), though comparisons are only valid for short distances from the radar (near ground). Also notice the sharp pressure spike attending the bore passage and the absence of any surface cooling – both being common characteristics of bores (Fig. 8a).

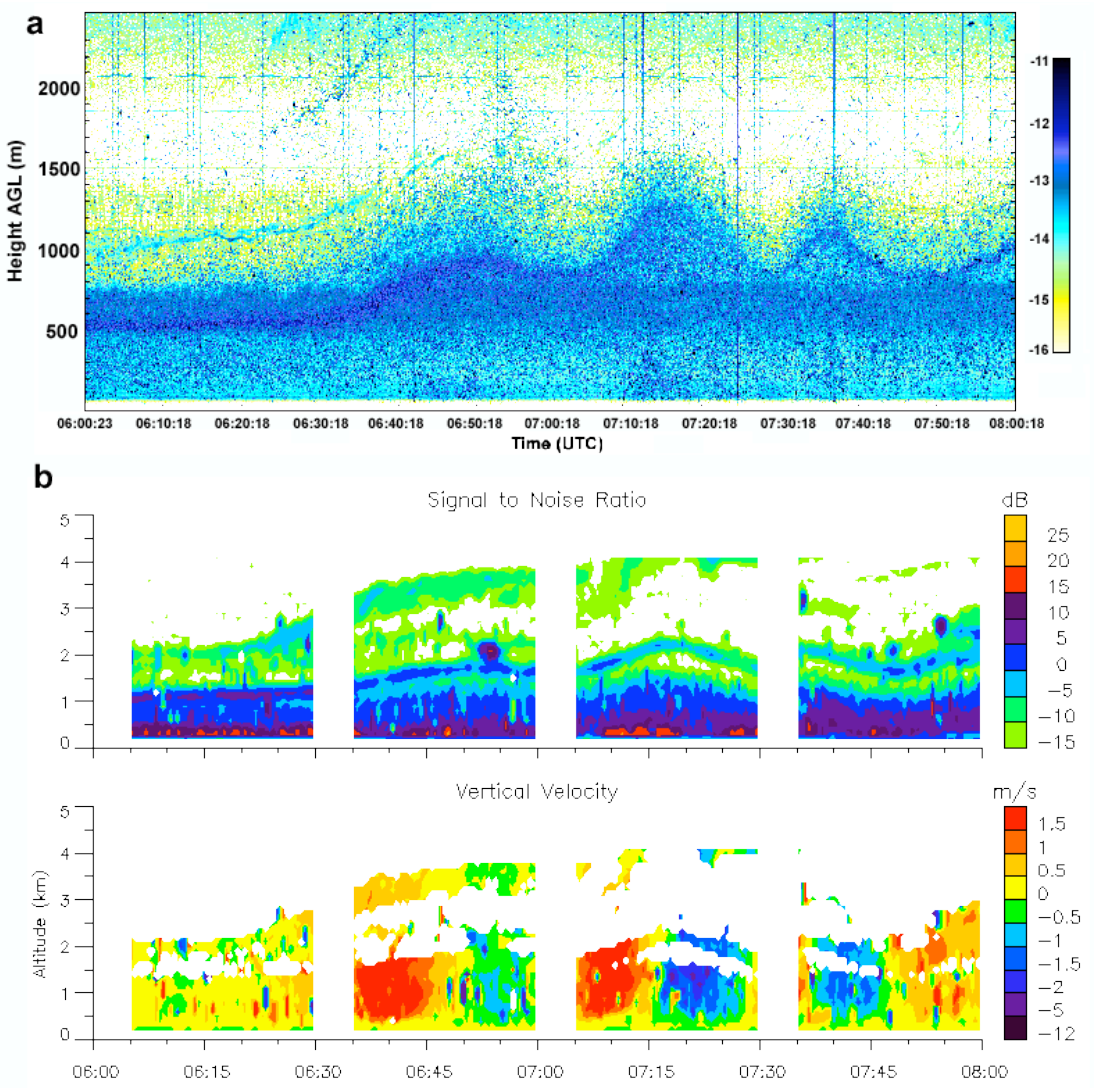

Fig. 4. Bore A on 4 June 2002 as observed by a) FM-CW (reflectivity, units of dBZ) and by b) MAPR. Middle panel shows MAPR SNR (dB), bottom panel shows measured vertical motions (m s^{-1}), with updrafts in red and downdrafts in blue. Bore front passes site at 0630 UTC, and results in a sustained SBL deepening followed by 2-3 solitary waves.

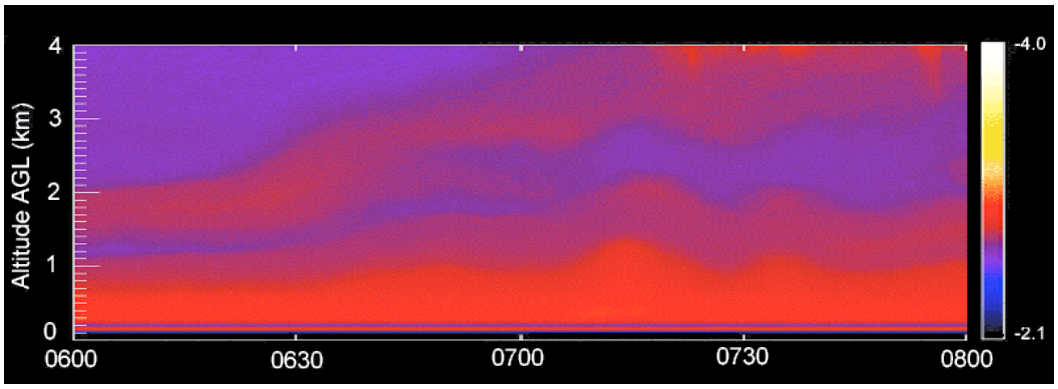

Fig. 5. Bore A as observed by HARLIE (0600 – 0800 UTC). Note the stratified structures in aerosols.

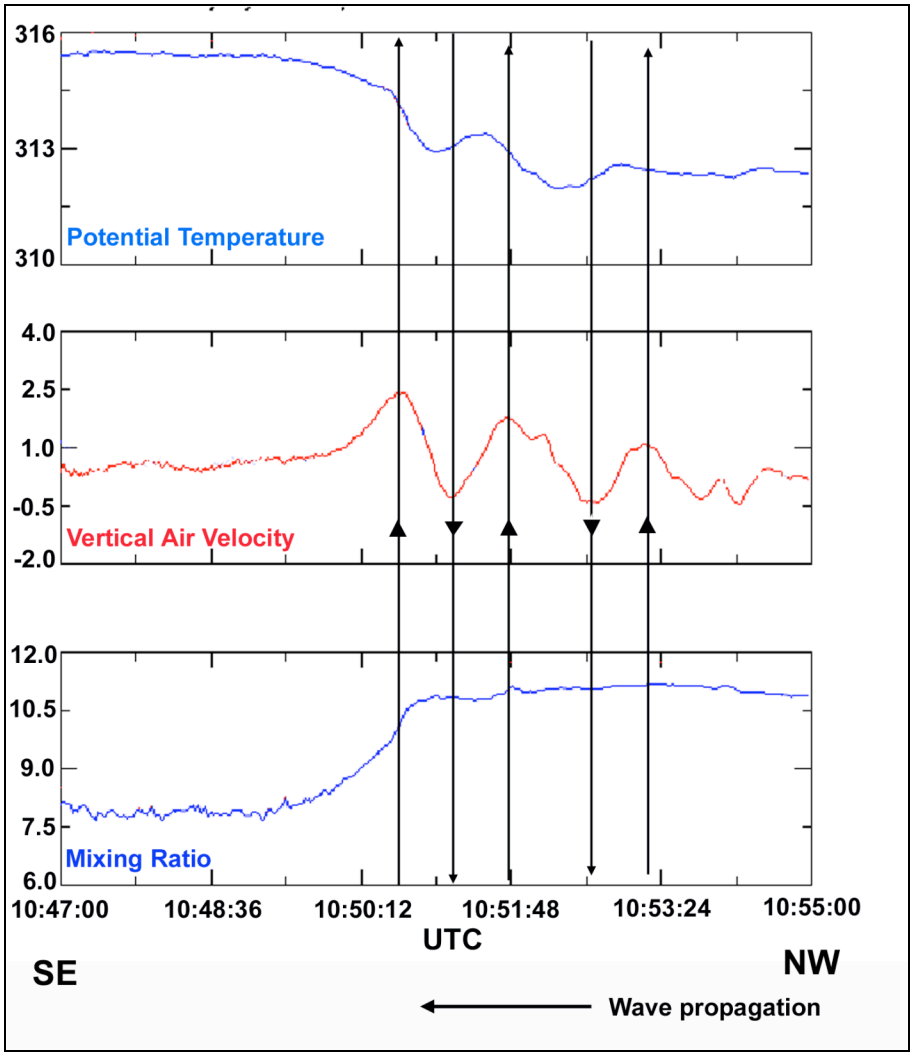

Fig. 6. Bore B and soliton as seen in UWKA aircraft in situ data at 1850 m AGL (at the height of the upper wave crests). Aircraft flew overpass through the soliton in a northwesterly direction opposed to the direction of propagation of the soliton. Fluctuations in potential temperature (K) follow those in vertical air velocity (m s^{-1}) by one-quarter of a wave period. Insignificant fluctuations appear in the mixing ratio data (g kg^{-1}), but a large increase in moisture does accompany passage through the bore system.

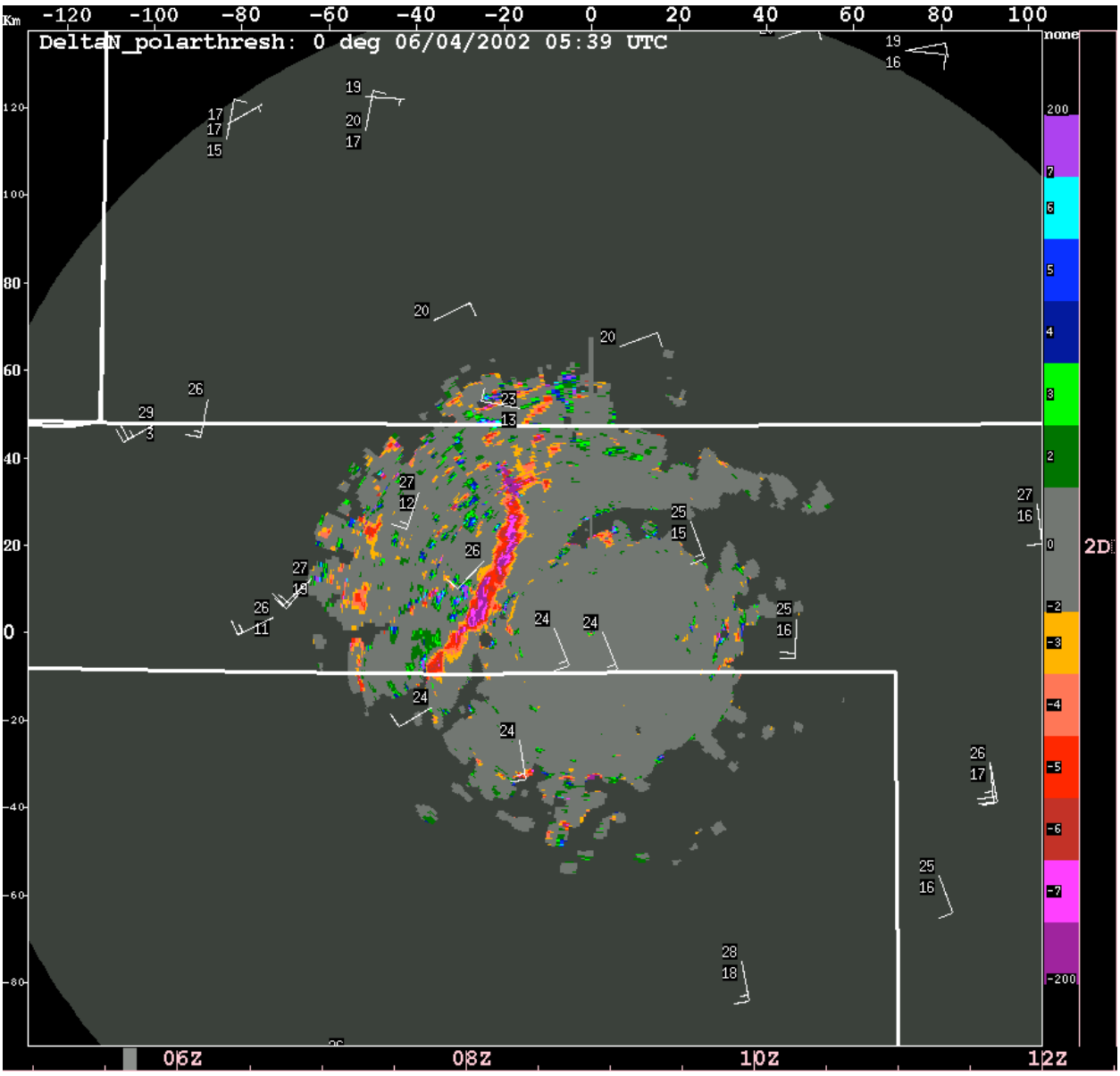

Fig. 7. Refractivity 12-min change field computed from S-POL measurements at 0539 UTC 4 June 2002 during passage of Bore A through the Homestead vicinity in the Oklahoma Panhandle (note white state borders). Local mesonetwork observations (temperature and dew point (°C) and winds (kt) are also shown. The bore is clearly located along the band of rapid decrease of refractivity within a zone of surface wind convergence.

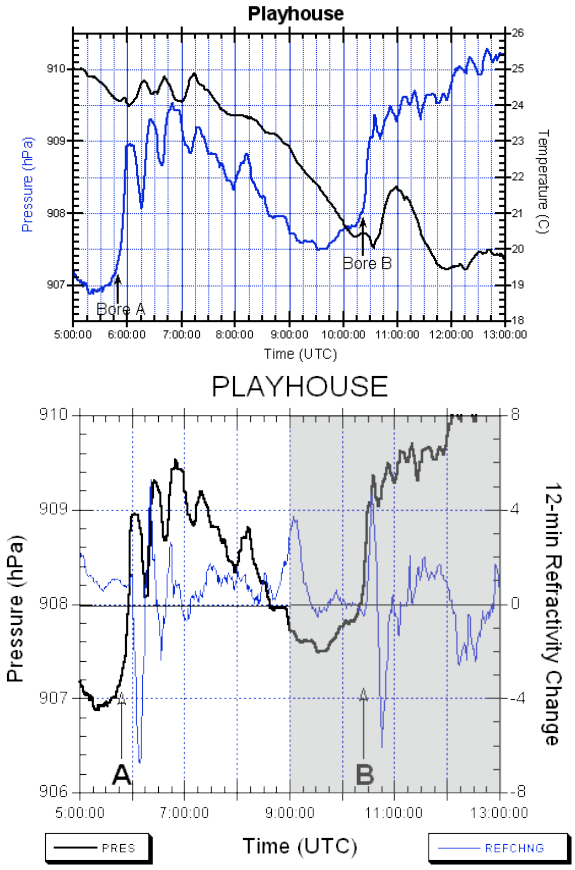

Fig. 8. Mesonetwork observations during the passage of bores A and B on 4 June 2002: a) surface pressure (hPa, blue) and temperature (°C, black), and b) refractivity 12-min change field computed from surface measurements (blue) and surface pressure (black). Playhouse is located within 5 km of the S-POL radar and other systems at Homestead. Note sharp decrease of 7 units of refractivity at 0615 UTC, in excellent comparison with that computed from the S-POL measurements (Fig. 7).

The observations were analyzed to predict the properties of gravity currents and bores for the 4 June events using the equations from hydraulic theory presented in section 2. The height of the tropopause was obtained from the 0430 UTC ISS sounding at Homestead. The value for the mean wind U was estimated from the MM5 simulations (Fig. 9a). Inversion and bore depth values were provided by the FM-CW data and the Homestead CLASS soundings at 0401 and 1046 UTC for bores A and B, respectively. The gravity current speed was estimated from the speed of propagation of the "fine line" seen on the S-POL and mesonetwork composite displays. The depth of the gravity current d_{gc} was derived from gravity current theory using the "observed" gravity current speed and assuming a value for the Froude Number of 0.9. The inversion strength value was taken from the Homestead soundings. Results shown below indicate that the observed gravity current and environmental stability structure supported bores of moderate strength. Observed and predicted bore speeds (the latter being an average of 5 different values from various hydraulic theories as explained in Koch and Clark (1999)) agree with one another to within 27% for bore A and within 5% for bore B.

Parameter (units)	Sym.	Bore A	Bore B
Tropopause (m)	H	12500	12500
Bore depth (m)	d_b	1200	1600
Inversion depth (m)	h_0	750	1000
Bore speed (m s^{-1}): observed	C_b	20.3	7.3
Inversion strength (K)	$\delta\theta$	10.0	3.0
Head wind (m s^{-1})	U	10.0	10.0
Bore strength	d_b / h_0	1.6	1.6
Gravity current depth (m)	d_0	1550	915
Normalized depth	d_0 / h_0	2.1	0.9
Gravity wave speed (m s^{-1})	C_{gw}	15.4	9.8
Current speed (m s^{-1})	C_{gc}	18.0	6.9
Froude number	Fr	1.2	0.7
Bore speed (m s^{-1}): predicted	C_b	14.8	6.9

7. Model simulations

The picture that emerges from the synthesis of the mesonet, S-POL, AERI, and UWKA data is one of drying and slight warming near the surface, with cooling and moistening aloft caused by the passage of the bores. This suggests the hypothesis that bores produce cooling through adiabatic lifting, that the moistening aloft is the result of venting of moist air in the near-surface air ahead of the bore upwards above the bore head, and that the drying and warming at the surface is caused by the turbulent entrainment of air from above the SBL down to the surface.

In order to test this hypothesis, it is necessary to perform a very high-resolution model simulation (in both the horizontal and vertical directions) with the capability to explicitly represent vertical mixing processes associated with individual solitary waves following the bore. Our attempt to do this with large-eddy simulation models failed to be successful, but we were able to obtain meaningful and surprisingly realistic

results with the 0.7-km nested grid model containing 22 levels in the lowest 1.5 km of the model, and using the BT PBL scheme (Fig. 9).

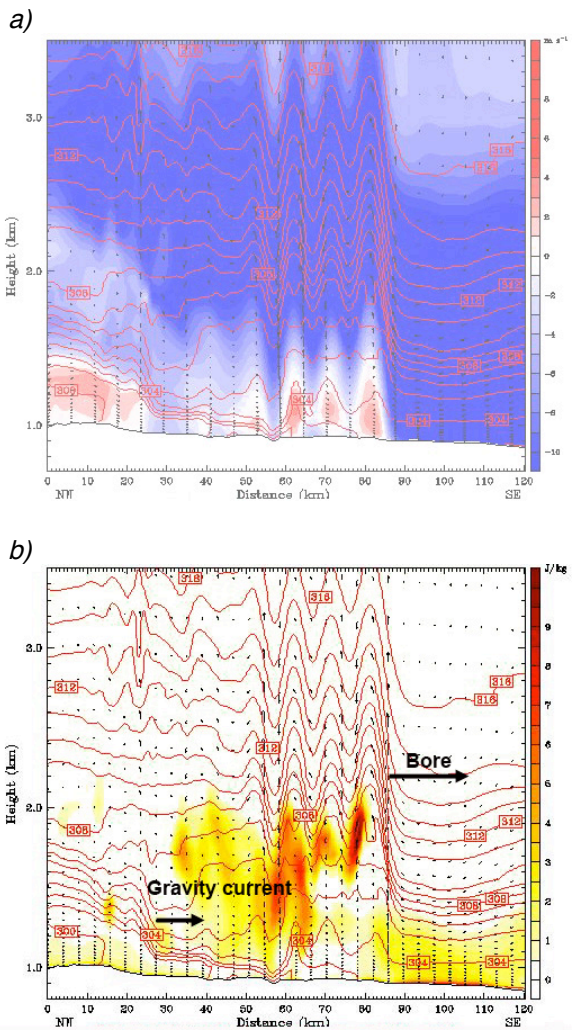

Fig. 9. MM5 model simulation of bore B from 9.17h forecast valid at 0910 UTC 4 June 2002. This 0.7-km nested grid simulation uses the BT PBL scheme and shows a) potential temperature (1K isentropic intervals), vertical motions, and magnitude of horizontal motions relative to the movement of the gravity current (which is at the left side of the domain), and b) Turbulent Kinetic Energy (J kg^{-1}, shaded) and isentropes.

These results show that not only did the model reproduce the gravity current and the four waves within the soliton for bore B, but also the characteristics of the wind and thermodynamic fields are surprisingly realistic. The waves are amplitude-ordered, with the leading wave (the bore head) being lifted 0.8 km and the following waves displaying only 0.2 km of lifting. The wavelength of 11 km compares with the 7 km (15 min x 7.3 m s^{-1}) seen in the FM-CW and MAPR observations (Fig. 10). Each of these solitary waves exhibits a localized region of positive flow (i.e., closed circulations), whereas the gravity current displays a broader feeder flow region (Fig. 9a). The magnitude of TKE (Fig. 9b) is largest at the bottom of each of the solitary waves, suggesting the ability of the waves to efficiently transport dry air from above the SBL deep down into the surface layer.

Animations of the model forecast fields revealed that solitary waves did not have their origin in a manner explainable by intrinsic wave dispersion in classical bore theory. Rather, "lee-wave" activity produced by strong jet-like flow over the bore head appeared to have generated trapped waves in the lee of the bores in a consecutive fashion. These results suggest that the existing theory may need to be revised.

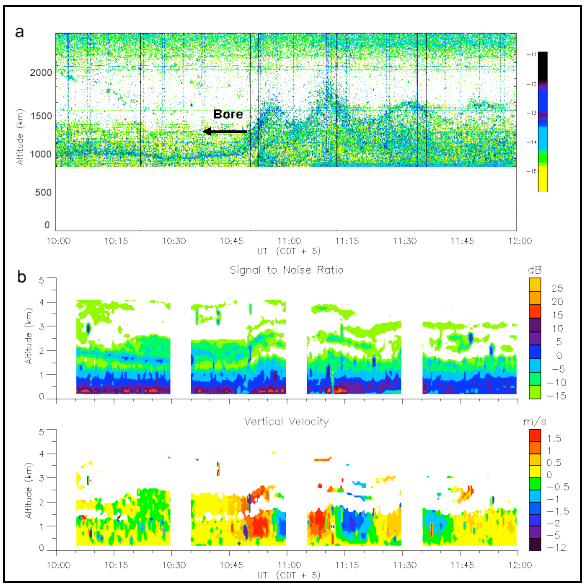

Fig. 10. Bore B on 4 June 2002 as observed by a) FM-CW radar (reflectivity, units of dBZ) and by b) MAPR. Middle panel shows MAPR SNR (dB), bottom panel shows measured vertical motions (m s^{-1}), with updrafts in red and downdrafts in blue. Bore front passes site at 1050 UTC, and results in a sustained SBL deepening followed by 2-3 solitary waves. Problems existed in FM-CW data below 0.7 km. Panels should be switched about a vertical axis with time increasing to the left in order to make a direct comparison with the model simulation results shown in Fig. 9.

8. Conclusions

Bores and solitons from three separate events in IHOP appeared as fine lines in S-POL reflectivity displays and their vertical structures were readily detected by the lidar and radar systems, allowing direct comparison with hydraulic theory predictions. S-POL and mesonetwork refractivity calculations indicated pronounced surface layer drying accompanied the passage of the bores due to downward turbulent mixing within the solitary waves, whereas the AERI and UWKA data indicated cooling and moistening occurred aloft as the result of lifting over the bore head. This suggestion was confirmed by the results of very high-resolution model simulations of one of the bores. The bores formed on a surface stable layer and multiple solitary waves developed from the bores in both the observations and the simulations. This inversion was lifted abruptly by the bore head and further by each passing wave, in a stair step fashion, thereby destabilizing the atmosphere. The synthesis of these unprecedented observations with high-resolution model simulations of the actual events (using nesting at a horizontal grid spacing of 0.7 km) indicate that solitary wave origin as explained by classical bore theory was not the general cause for the waves. Rather, "lee-wave" activity produced by strong jet-like flow over the bore head appeared to have generated the waves in the lee of the bores, suggesting a substantial modification to the existing theory is needed.

The origin of the bores has not been fully determined from these data. Differences in wave characteristics (wavelength, number, etc.) and inversion layer details existing between the observing systems require explanation. It is unknown why the number of waves within the soliton varied with the life cycle of the bore. The actual cause(s) for the observed changes in the refractivity fields seen from S-POL and the mesonet data are also unclear at this time. Future plans include the need to understand the nature of the entrainment process in the presence of strong solitary waves. It would also be desirable to merge the MAPR, S-POL radial velocity, and GLOW wind data to obtain a complete wind field associated with the bores and solitary waves, from which a quantitative comparison could be made with the FM-CW, MAPR, and DIAL measurements of stable layer changes caused by the bores.

9. References

Bruneau, D., P. Quaglia, C. Flamant, M. Meissonnier, and J. Pelon, 2001: Airborne lidar LEANDRE II for water-vapor profiling in the troposphere. *Applied Optics*, **40,** 3450–3475.

Burk, S. D., and W. T. Thompson, 1989: A vertically nested regional numerical weather prediction model with second-order closure physics. *Mon. Wea. Rev.,* **117,** 2305–2324.

Christie, D.R., K.J. Muirhead and A.L. Hales, 1979: Intrusive density flows in the lower troposphere: A source of atmospheric solitons. *J. Geophys. Res.*, **84,** 4959–4970.

Christie, D.R., 1989: Long nonlinear waves in the lower atmosphere. *J. Atmos. Sci.,* **46,** 1462–1491.

Cohn, S.A., et. al., 2001: Clear air boundary layer spaced antenna wind measurement with the Multiple Antenna Profiler (MAPR), *Annales Geophysicae*, **19,** 845–854.

Crook, N. A., 1988: Trapping of low-level internal gravity waves. *J. Atmos. Sci.,* **45,** 1533-1541.

Demoz, B., et al., 2003: Lidar measurements of wind, moisture, and boundary layer evolution in a dryline during IHOP2002. Preprints, *Symposium on Variability of Water in Weather and Climate*, Long Beach, Amer. Meteor. Soc.

Droegemeier, K. K., and R. B. Wilhelmson, 1985: Three-dimensional numerical modeling of convection produced by interacting thunderstorm outflows. Part I: Control simulation and low-level moisture variations. *J. Atmos. Sci.*, **42,** 2381–2403.

Fabry, F., C. Frush, I. Zawadzki and A. Kilambi, 1997: On the extraction of near-surface index of refraction using radar phase measurements from ground targets. *J. Atmos. Oceanic Technol.*, **14,** 978–987.

Feltz, W. F., H. B. Howell, R. O. Knuteson, H. M. Woolf, and H E. Revercomb, 2003: Near continuous profiling of temperature, moisture, and atmospheric stability using the Atmospheric Emitted Radiance Interferometer (AERI). *J. Appl. Meteor.*, **42,** 584-597.

Fulton, R., D. S. Zrnic, and R.J. Doviak, 1990: Intiation of a solitary wave family in the demise of a nocturnal thunderstorm density current. *J. Atmos. Sci.,* **47,** 319–337.

Gentry, B. M., H. Chen, and S. X. Li, 2000: Wind measurements with a 355 nm molecular Doppler lidar, *Optics Letters*, **25,** 1231–1233.

Haase, S. P., and R.K. Smith, 1989a: The numerical simulation of atmospheric gravity currents. Part I: Neutrally–stable environments. *Geophys. Astrophys. Fluid Dynamics*, **46,** 1–33.

_____, 1989b: The numerical simulation of atmospheric gravity currents. Part II: Environments with stable layers. *Geophys. Astrophys. Fluid Dynamics,* **46,** 35–51.

Ince, T., A.L. Pazmany, S.J. Frasier, and R.E. McIntosh, 1998: A high resolution FM-CW S-band radar for boundary layer profiling and cloud applications. Proceedings of the 1998 *Battlespace Atmospherics Conference,* Hanscom AFB, MA, Dec. 1-3, 1998, 432–439.

Janjic, Z. I., 1994: The step-mountain Eta coordinate model: Further developments of the convection, viscous sublayer, and turbulence closure schemes. *Mon. Wea. Rev.,* **122,** 927–945.

Jin, Y., S. E. Koch, Y.–L. Lin, F. M. Ralph, and C. Chen, 1996: Numerical simulations of an observed gravity current and gravity waves in an environment characterized by complex stratification and shear. *J. Atmos. Sci.,* **53,** 3570–3588.

Klemp, J. B., R. Rotunno, and W. C. Skamarock, 1997: On the propagation of internal bores. *J. Fluid Mech.,* **331,** 81–106.

Koch, S. E., et. al., 1991: Structure of an internal bore and dissipating gravity current as revealed by Raman Lidar. *Mon. Wea. Rev.,* **119,** 857–887.

Koch, S. E., and W. Clark, 1999: A nonclassical cold front observed during COPS-91: Frontal structure and the process of severe storm initiation. *J. Atmos. Sci.,* **56,** 2862-2890.

Locatelli, J. D., M. T. Stoelinga, P. V. Hobbs, and J. Johnson, 1998: Structure and evolution of an undular bore on the High Plains and its effects on migrating birds. *Bull. Amer. Meteor. Soc.,* **79,** 1043–1060.

Lutz, J., et. al., 1995: NCAR's S-Pol: Portable polarimetric S-band radar. Preprints, *Ninth Symp. on Meteorological Observations and Instrumentation*, Charlotte, NC, Amer. Meteor. Soc., 408–410.

Maxworthy, T., 1980: On the formation of nonlinear internal waves from the gravitational collapse of mixed regions in two and three dimensions. *J. Fluid Mech.,* **96,** 47–64.

Mueller, C. K., and R. E. Carbone, 1987: Dynamics of a thunderstorm outflow. *J. Atmos. Sci.*, **44,** 1879–1898.

Rottman, J.W., and J.E. Simpson, 1989: The formation of internal bores in the atmosphere: A laboratory model. *Quart. J. Roy. Meteor. Soc.*, **115,** 941–963.

Schwemmer, G., T. Wilkerson, and D. Guerra, 1998: Compact scanning lidar systems using holographic optics. *SPIE Conf. Optical Remote Sensing for Industry and Environmental Monitoring*, Beijing, China.

Simpson, J. E., 1987: *Gravity Currents: in the Environment and the Laboratory*. Wiley & Sons, 244 pp.

Weckwerth, T. M., D. B. Parsons, S. E. Koch, J. A. Moore, M. A. LeMone, B. B. Demoz, C. Flamant, B. Geerts, J. Wang, and W. F. Feltz, 2004: An overview of the International H20 Project (IHOP_2002) and some preliminary highlights. *Bull. Amer. Meteor. Soc.*, **85,** 253-277.